

Buckling Behavior of Composite Triangular Plates

T. Farsadi , E. Heydarnia and P. Amani
Aerospace Engineering Department, Sharif University of Technology, Tehran, Iran

ABSTRACT: This paper is to do a brief research on the buckling behavior of composite triangular plates with various edge boundary conditions and in-plane loads. It may be regarded as a right and simple numerical method for the analysis of composite triangular thin plate using the natural Area coordinates. Previous studies on the solution of triangular plates with different boundary conditions were mostly based on the Rayleigh-Ritz principle which is performed in the Cartesian coordinate. In this method, the energy functional of a general triangular plate is derived and the Rayleigh-Ritz method is utilized to derive the governing eigenvalue equation for the buckling problem. The geometry is presented in a natural way by mapping a parent triangle and the integrals are evaluated analytically. The polynomial terms in the Area coordinates are employed to interpolate plate deflection. In this approach, the convergence is always assured due to the completeness of interpolating polynomials. Extensive buckling factors are presented for several selected right-angled and isosceles triangular plates of various edge support conditions and subjected to composite thin plates under various in-planes compressive loads and the results are validated to the other results.

Keywords: Triangular plate - Composite material - Area coordinate - Rayleigh-Ritz principle - Buckling

1 INTRODUCTION

In many engineering applications such as isogrid structures (waffle plates), reinforced plates or panels, aero-structures, ... , it is very important to predict buckling behavior of triangular plates. Buckling phenomenon is critically dangerous to structural components because the buckling of plates usually occurs at a lower applied stress and generates large deformation. This led to a focus on the study of buckling behavior in plates or panels. The use of composite materials in place of more traditional isotropic materials has increased dramatically over the past decades in areas such as the civil and aerospace industry. With the wide use of composite plate structures in modern industries, dynamic and static analysis of plates of complex geometry becomes an important part of engineering design. Composite materials have been widely used due to their excellent high strength-to-weight ratio, modulus-to-weight ratio and the controllability of the structural properties with variation of fiber orientation. The problem regarding buckling of plates under various shapes and boundary conditions has been studied in some famous classic and academic reference text books [1,2] and some of numerous literature works [3-6]. It is interesting to note that buckling of triangular plates has received far less attention than their rectangular counterparts. Woinowsky-Krieger [7] derived the exact buckling load for a simply supported equilateral triangular plate under an isotropic in-plane compressive load. Burchard [8] studied the buckling of simply supported right-angled triangular plates under uni-axial compression. There are several researches investigated the buckling of isosceles triangular plates under various loading conditions. Wakasugi [9,10] investigated the buckling of simply -

supported and clamped equilateral triangular plates. Conway and Leissa [11] searched the buckling of equilateral triangular plates subjected to isotropic in-plane compression. Tan et al. [12] and Tan [13] employed the finite element method to study the buckling of general triangular plates. In the recent years, Wang and Liew [14] utilized their pb-2 Rayleigh-Ritz method to investigate the buckling of isosceles and right-angled triangular plates under isotropic in-plane compressive load.

The basic aim of this research is to study and formulate the effect of plate geometry aspect ratio and fiber orientation to determine critical value of buckling load factor for a composite triangular plate of various boundary conditions and various in-plane (compression and shear) loads by using an approximate-analytical solution for first critical mode predominantly.

2 THEORETICAL FORMULATION

2.1 Area Coordinate

In this section, the use of triangular coordinates to define the interior of a triangular area is briefly described. This description is important when formulating triangular finite elements. The triangle in Fig. 1 is defined by coordinates (x_i, y_i) of its vertices in the coordinate system $O(x, y)$. Cartesian coordinates are usually employed to describe any point (x_0, y_0) on a rectangular area. They are, however, difficult to use when the boundary and the interior of a triangular area need to be defined. In order to define a triangular area, the coordinates (x_0, y_0) can be expressed in the following way,

$$\begin{cases} x = x_1L_1 + x_2L_2 + x_3L_3 \\ y = y_1L_1 + y_2L_2 + y_3L_3 \end{cases} \quad (1)$$

where L_1, L_2, L_3 are triangular coordinates. The values of the triangular coordinate range between 0 and 1 when the following constraint is used,

$$L_1 + L_2 + L_3 = 1 \quad (2)$$

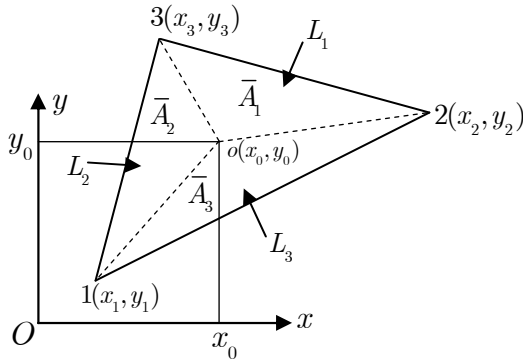


Fig. 1. Area coordinates in arbitrary triangular plate

Equation (1) together with (2) can be used to define any point (x_0, y_0) in the triangle. The coordinates L_1, L_2, L_3 represent dimensionless areas of triangles $\bar{A}_1, \bar{A}_2, \bar{A}_3$ as depicted in Fig. 1. These coordinates can be expressed as follows:

$$\begin{cases} \bar{A}_1 + \bar{A}_2 + \bar{A}_3 = A \\ L_i = \frac{\bar{A}_i}{A}, \quad i = 1, 2, 3 \end{cases} \quad (3)$$

where A is the area of the triangle defined as,

$$2A = \begin{vmatrix} x_1 & x_2 & x_3 \\ y_1 & y_2 & y_3 \\ 1 & 1 & 1 \end{vmatrix} \quad (4)$$

when constraint (2) is accounted for, the triangular coordinates can be solved from (5) as follows,

$$L_i = \frac{1}{2A}(\alpha_i + \beta_i x + \gamma_i y), \quad i = 1, 2, 3 \quad (5)$$

Where α_i a coefficient that depends on is coordinates x_j, y_k of the three nodes in the coordinate system $O(x, y)$. The coefficients can be expressed as follows,

$$\begin{cases} \alpha_i = x_j y_k - y_j x_k, & \beta_i = y_j - y_k, \\ \gamma_i = x_k - x_j, & j, k = 1, 2, 3 \end{cases} \quad (6)$$

In the latter equation and below j, k and i form a cyclic permutation.

Thin plate theory is used in the present analysis. However, to obtain the strains differentiation operator with respect to Cartesian coordinates needs to be carried out. This is done as follows,

$$\begin{aligned} \frac{\partial}{\partial x} &= \sum_{i=1}^3 \frac{\partial}{\partial L_i} \frac{\partial L_i}{\partial x} = \frac{1}{2A} \sum_{i=1}^3 \beta_i \frac{\partial}{\partial L_i} \\ \frac{\partial}{\partial y} &= \sum_{i=1}^3 \frac{\partial}{\partial L_i} \frac{\partial L_i}{\partial y} = \frac{1}{2A} \sum_{i=1}^3 \gamma_i \frac{\partial}{\partial L_i} \\ \frac{\partial^2}{\partial x^2} &= \frac{\partial}{\partial x} \frac{\partial}{\partial x} = \frac{1}{4A^2} \sum_{i=1}^3 \sum_{j=1}^3 \beta_i \beta_j \frac{\partial}{\partial L_i} \frac{\partial}{\partial L_j} \\ \frac{\partial^2}{\partial y^2} &= \frac{\partial}{\partial y} \frac{\partial}{\partial y} = \frac{1}{4A^2} \sum_{i=1}^3 \sum_{j=1}^3 \gamma_i \gamma_j \frac{\partial}{\partial L_i} \frac{\partial}{\partial L_j} \\ \frac{\partial^2}{\partial x \partial y} &= \frac{\partial}{\partial x} \frac{\partial}{\partial y} = \frac{1}{4A^2} \sum_{i=1}^3 \sum_{j=1}^3 \beta_i \gamma_j \frac{\partial}{\partial L_i} \frac{\partial}{\partial L_j} \end{aligned} \quad (7)$$

All expressions remain polynomial in the Area coordinates and can be easily integrated.

In other words,

$$\begin{bmatrix} \frac{\partial}{\partial x} \\ \frac{\partial}{\partial y} \end{bmatrix} = [R] \begin{bmatrix} \frac{\partial}{\partial L_1} \\ \frac{\partial}{\partial L_2} \\ \frac{\partial}{\partial L_3} \end{bmatrix}, \quad \begin{bmatrix} \frac{\partial^2}{\partial x^2} \\ \frac{\partial^2}{\partial y^2} \\ \frac{\partial^2}{\partial x \partial y} \end{bmatrix} = [Q] \begin{bmatrix} \frac{\partial^2}{\partial L_1^2} \\ \frac{\partial^2}{\partial L_2^2} \\ \frac{\partial^2}{\partial L_3^2} \\ \frac{\partial^2}{\partial L_1 \partial L_2} \\ \frac{\partial^2}{\partial L_2 \partial L_3} \\ \frac{\partial^2}{\partial L_1 \partial L_3} \end{bmatrix} \quad (8)$$

where,

$$[R] = \frac{1}{2A} \begin{bmatrix} \beta_1 & \beta_2 & \beta_3 \\ \gamma_1 & \gamma_2 & \gamma_3 \end{bmatrix} \quad (9)$$

$$[Q] = \frac{1}{4A^2} \begin{bmatrix} \beta_1^2 & \beta_2^2 & \beta_3^2 \\ \gamma_1^2 & \gamma_2^2 & \gamma_3^2 \\ 2\beta_1\gamma_1 & 2\beta_2\gamma_2 & 2\beta_3\gamma_3 \\ \beta_1\beta_2 & \beta_2\beta_3 & \beta_3\beta_1 \\ \gamma_1\gamma_2 & \gamma_2\gamma_3 & \gamma_3\gamma_1 \\ (\beta_1\gamma_2 + \gamma_1\beta_2) & (\beta_2\gamma_3 + \gamma_2\beta_3) & (\beta_3\gamma_1 + \gamma_3\beta_1) \end{bmatrix} \quad (10)$$

$[R]$ and $[Q]$ are transfer matrices.

2.2 The Displacement Vector Field

For the displacement field in L_1, L_2 and L_3 the Area coordinate system is used for the function as follows,

$$\begin{cases} w = w_u w_v \\ w_u = w_u(L_1, L_2, L_3), \quad w_v = w_v(L_1, L_2, L_3) \end{cases} \quad (11)$$

$w_u(L_1, L_2, L_3)$ is taken as the product of the boundary equations and the internal line/curved support equations and $w_v(L_1, L_2, L_3)$ is a polynomial in the Area coordinates with an undetermined coefficient that the holder of the displacement field is expanded. The $w_u(L_1, L_2, L_3)$ function is defined,

$$w_u = L_1^a L_2^b L_3^c \quad (12)$$

where the value a, b, c depending on the free, simply supported or clamped boundary conditions are 0, 1 or 2.

$w_v(L_1, L_2, L_3)$ shape function includes terms with unknown coefficients ψ_{ijk} as follow,

$$\begin{cases} w_{vI} = \sum_{i=0}^p \sum_{j=0}^p \sum_{k=0}^p \psi_{ijk} L_1^i L_2^j L_3^k, \\ i + j + k = p, \quad 0 \leq i, j, k \leq p \end{cases} \quad (13)$$

So that the polynomial order p and i, j, k , respectively, display the correct coordinates L_1, L_2, L_3 , varies from zero to p . $w_v(L_1, L_2, L_3)$, shape function can be demonstrated with uncertainty factor that is just an index as follows. Such a display of computer programming is essential for the shape function, $w_v(L_1, L_2, L_3)$

$$w_{vI} = \sum_{I=1}^N \Psi_I L_1^i L_2^j L_3^k \quad (14)$$

where "I" is number of sentences and N is the count of sentences. Performing some mathematical operations can be shown that a simple choice for the i, j, k using the following equation,

$$\begin{cases} i = I - jN - kN^2 - 1 \\ j = INT \left(\frac{I - 1 - kN^2}{N} \right) \\ k = INT \left(\frac{I - 1}{N^2} \right) \end{cases} \quad (15)$$

second shape function is obtained by,

$$w_{vJ} = \sum_{J=1}^N \Psi_J L_1^e L_2^f L_3^g \quad (16)$$

where,

$$\begin{cases} e = J - fN - gN^2 - 1 \\ f = INT \left(\frac{J - 1 - eN^2}{N} \right) \\ g = INT \left(\frac{J - 1}{N^2} \right) \end{cases} \quad (17)$$

and the count sentences is possible by the following equation,

$$N = \frac{1}{2}(p+1)(p+2) \quad (18)$$

and thus specifying the order of the polynomial p and the number of sentence can get symbols i, j, k with number of sentence "I".

2.3 The Rayleigh-Ritz Method

The Rayleigh-Ritz method consists of assuming that some desired deflection pattern can be approximated by a linear combination of deflection functions, each of which satisfied the rigid boundary conditions of the problem, and then finding the coefficients governing this linear combination by minimizing the total energy of the deformed body and the in-plane loads. Clearly, a proper choice of the deflection expression is important to ensure good accuracy for the final solution. The total energy is the sum of the strain energy of the plate, U , and the potential energy of the in-plane loads, V .

3 GOVERNING EQUATIONS

In this paper, an elastic, composite, flat and thin triangular plate is used. The edges of the plate may be free, simply supported or clamped supported. The boundary of this plate defined by the equations $L_1 = 0, L_2 = 0, L_3 = 0$ and the boundary conditions are provided by choosing a, b, c . It is noteworthy that even if x and y axes are not coincided with the main purpose, there is no limit to the formulation. The problem at hand is to determine the buckling behavior of composite triangular plates with various edge boundary conditions and in-plane compressive loads.

In accordance with established stiffness procedures, the vector of infinitesimal buckling strains consists of two parts. (i) The linear flexural strain ε_L , and (ii) the nonlinear flexural strain ε_N , that are given by,

$$\begin{cases} \{\varepsilon_L\} = \{\varepsilon_{Lx}, \varepsilon_{Ly}\}^T \\ = \left\{ \left(\frac{\partial w}{\partial x} \right)^2, \left(\frac{\partial w}{\partial y} \right)^2 \right\}^T \\ \{\varepsilon_N\} = \{\varepsilon_{Nx}, \varepsilon_{Ny}, \varepsilon_{Nxy}\}^T \\ = \left\{ \frac{\partial^2 w}{\partial x^2}, \frac{\partial^2 w}{\partial y^2}, \frac{2\partial^2 w}{\partial x \partial y} \right\}^T \end{cases} \quad (19)$$

Infinitesimal buckling Linear and Nonlinear strains in an Area coordinate system are defined,

$$\begin{cases} \{\widehat{\varepsilon}_L\} = \{\varepsilon_{L1}, \varepsilon_{L2}, \varepsilon_{L3}\}^T \\ = \left\{ \left(\frac{\partial w}{\partial L_1} \right)^2, \left(\frac{\partial w}{\partial L_2} \right)^2, \left(\frac{\partial w}{\partial L_3} \right)^2 \right\}^T \\ \{\widehat{\varepsilon}_N\} = \{\varepsilon_{N1}, \varepsilon_{N2}, \varepsilon_{N3}, \varepsilon_{N12}, \varepsilon_{N23}, \varepsilon_{N31}\}^T \\ = \left\{ \frac{\partial^2 w}{\partial L_1^2}, \frac{\partial^2 w}{\partial L_2^2}, \frac{\partial^2 w}{\partial L_3^2}, \frac{\partial^2 w}{\partial L_1 \partial L_2}, \frac{\partial^2 w}{\partial L_2 \partial L_3}, \frac{\partial^2 w}{\partial L_3 \partial L_1} \right\}^T \end{cases} \quad (20)$$

between vectors $\{\varepsilon_L\}$, $\{\widehat{\varepsilon}_L\}$ and $\{\varepsilon_N\}$, $\{\widehat{\varepsilon}_N\}$ using the relationship between Cartesian coordinates and the Area coordinates are expressed as the following,

$$\begin{cases} \{\varepsilon_L\} = [R]\{\widehat{\varepsilon}_L\} \\ \{\varepsilon_N\} = [Q]\{\widehat{\varepsilon}_N\} \end{cases} \quad (21)$$

so that transfer matrix $[R]$, $[Q]$ with fixed array is calculated and available in (8).

3.1 Strain Energy

Adopting the classical thin plate theory, the strain energy U due to bending is given in the matrix form, by,

$$U = \iint_{A/2} \frac{1}{2} \{\varepsilon_N\}^T [D] \{\varepsilon_N\} dA \quad (22)$$

where "D" is the standard matrix of elastic constants for single layer composite plate transformed to the local element coordinate system and is given by,

$$[\overline{D}] = \begin{bmatrix} d_{11} & d_{12} & 0 \\ d_{12} & d_{22} & 0 \\ 0 & 0 & d_{33} \end{bmatrix} \quad (23)$$

where,

$$\begin{cases} d_{11} = \frac{t^3}{12} \frac{E_1}{(1 - \nu_{12}\nu_{21})}, d_{12} = \frac{t^3}{12} \frac{\nu_{12}E_2}{(1 - \nu_{12}\nu_{21})} \\ d_{22} = \frac{t^3}{12} \frac{E_2}{(1 - \nu_{12}\nu_{21})}, d_{33} = \frac{t^3}{12} G_{12} \end{cases} \quad (24)$$

In the above expressions, E_1 , E_2 , ν_{12} , ν_{21} , and G_{12} are elastic constants dependent on the physical characteristics of the plate material. For the composite material, the fiber orientation of the major direction of a lamina is defined by θ which is the anticlockwise angle from the positive x -direction (see Fig. 2). Then, transform matrix is defined by,

$$[T] = \begin{bmatrix} \cos^2 \theta & \sin^2 \theta & -2 \cos \theta \sin \theta \\ \sin^2 \theta & \cos^2 \theta & 2 \cos \theta \sin \theta \\ \cos \theta \sin \theta & -\cos \theta \sin \theta & \cos^2 \theta - \sin^2 \theta \end{bmatrix} \quad (25)$$

and elastic constant matrix is obtained by,

$$[D] = [T][\overline{D}][T]^T \quad (26)$$

by transfer elasticity matrix into Area coordinate and substituting (21) and (26) into (22), the strain energy U due to bending in Area coordinate is given by,

$$U = \iint_{A/2} \frac{1}{2} \{\widehat{\varepsilon}_N\}^T [\widehat{D}] \{\widehat{\varepsilon}_N\} dA \quad (27)$$

where,

$$[\widehat{D}] = [Q]^T [D] [Q] \quad (28)$$

function w using the following (11), (12), (13) and (14) are available,

$$\begin{cases} w_I = w_u w_{vI} = \langle \Phi_I(L_1, L_2, L_3) \rangle \{\Psi_I\}, \\ \Phi_I = L_1^{a+i} L_2^{b+j} L_3^{c+k} \end{cases} \quad (29)$$

and for second shape function,

$$\begin{cases} w_J = w_u w_{vJ} = \langle \Phi_J(L_1, L_2, L_3) \rangle \{\Psi_J\}, \\ \Phi_J = L_1^{a+e} L_2^{b+f} L_3^{c+g} \end{cases} \quad (30)$$

By substituting (29) and (30) into (27), strain energy in Area coordinate is given by,

$$U = \{\Psi\}^T \iint_{A/2} \frac{1}{2} \{P\}^T [\widehat{D}] \{P\} dA \{\Psi\} \quad (31)$$

In other words,

$$U = \frac{1}{2} \sum_I \sum_J K_{IJ} \Psi_I \Psi_J \quad (32)$$

so that,

$$K_{IJ} = \iint_{A/2} \{P\}_I^T [\widehat{D}] \{P\}_J dA \quad (33)$$

where,

$$\{P\}_{I(6 \times 1)} = \begin{bmatrix} (a+i)(a+i-1)L_1^{(a+i-2)} L_2^{(b+j)} L_3^{(c+k)} \\ (b+j)(b+j-1)L_1^{(a+i)} L_2^{(b+j-2)} L_3^{(c+k)} \\ (c+k)(c+k-1)L_1^{(a+i)} L_2^{(b+j)} L_3^{(c+k-2)} \\ 2(a+i)(b+j)L_1^{(a+i)} L_2^{(b+j-1)} L_3^{(c+k-1)} \\ 2(b+j)(c+k)L_1^{(a+i-1)} L_2^{(b+j)} L_3^{(c+k-1)} \\ 2(c+k)(a+i)L_1^{(a+i-1)} L_2^{(b+j)} L_3^{(c+k-1)} \end{bmatrix} \quad (34)$$

$\{P\}_{J(6 \times 1)} = \{P(a, b, c, e, f, g)\}$ is obtained similarly.

Provided that the arrays of matrix $\{P\}$ if the exponent is characteristics a negative, to be chosen as absolutely zero.

3.2 Potential Energy

The potential energy V of the orthotropic in-plane compressive and shear load can be expressed in the matrix form, as,

$$V = \iint_{A/2} \frac{1}{2} \{\varepsilon_L\}^T [N] \{\varepsilon_L\} dA \quad (35)$$

While $[N]$ contains the in-plane compressive and shear loads in the manner,

$$[N] = \begin{bmatrix} N_x & N_{xy} \\ N_{xy} & N_y \end{bmatrix} \quad (36)$$

In the above expressions, N_x , N_y and N_{xy} are in-plane compressive and shear load. By conversion load matrix into Area coordinate and substituting (21) and (36) into (35), the potential energy V due to bending in Area coordinate is given by,

$$V = \iint_{A/2} \frac{1}{2} \{\widehat{\varepsilon}_L\}^T [\widehat{N}] \{\widehat{\varepsilon}_L\} dA \quad (37)$$

where,

$$[\widehat{N}] = [R]^T [N] [R] \quad (38)$$

function w using the following (11), (12), (13) and (14) are available,

$$\begin{cases} w_I = w_u w_{vI} = \langle \Phi_I(L_1, L_2, L_3) \rangle \{ \Psi_I \}, \\ \Phi_I = L_1^{a+i} L_2^{b+j} L_3^{c+k} \end{cases} \quad (39)$$

and,

$$\begin{cases} w_J = w_u w_{vJ} = \langle \Phi_J(L_1, L_2, L_3) \rangle \{ \Psi_J \}, \\ \Phi_J = L_1^{a+e} L_2^{b+f} L_3^{c+g} \end{cases} \quad (40)$$

by substituting (39) and (40) into (37), potential energy in Area coordinate is given by,

$$V = \{ \Psi \}^T \iint_A \frac{1}{2} \{ Z \}^T [\hat{N}] \{ Z \} dA \{ \Psi \} \quad (41)$$

In other words,

$$V = \frac{1}{2} \sum_I \sum_J G_{IJ} \Psi_I \Psi_J \quad (42)$$

so that,

$$G_{IJ} = \iint_A \{ Z \}_I^T [\hat{N}] \{ Z \}_J dA \quad (43)$$

where,

$$\{ Z \}_{I(3 \times 1)} = \begin{Bmatrix} (a+1)L_1^{(a+i-1)} L_2^{(b+j)} L_3^{(c+k)} \\ (b+j)L_1^{(a+i)} L_2^{(b+j-1)} L_3^{(c+k)} \\ (c+k)L_1^{(a+i)} L_2^{(b+j)} L_3^{(c+k-1)} \end{Bmatrix} \quad (44)$$

$\{ Z \}_{J(6 \times 1)} = \{ Z(a, b, c, e, f, g) \}$ is obtained similarly.

It can be shown that when integrating polynomials in L_1, L_2 and L_3 over a triangle area A , the following relation holds,

$$\iint_A L_1^a L_2^b L_3^c dA = \frac{a!b!c!}{(a+b+c+2)!} 2A \quad (45)$$

3.3 Total Energy

Finally, with the function of both strain energy and the potential energy of the total energy is written as,

$$\begin{cases} \Pi = U - V \\ = \{ \Psi \}^T \iint_A \frac{1}{2} \{ P \}^T [\hat{D}] \{ P \} dA \{ \Psi \} - \\ \{ \Psi \}^T \iint_A \frac{1}{2} \{ Z \}^T [\hat{N}] \{ Z \} dA \{ \Psi \} \end{cases} \quad (46)$$

In other words,

$$\Pi = \frac{1}{2} \sum_I \sum_J (K_{IJ} \Psi_I \Psi_J - G_{IJ} \Psi_I \Psi_J) \quad (47)$$

3.4 Linear Buckling Analysis

Linear buckling technique allows one to obtain just the critical load and the corresponding deformed shape of the modeled structure. To obtain this result, the condition of neutral equilibrium between external loads and internal reactions is searched, solving the equation,

$$([K] - \lambda[G]) \{ \Psi \} = \{ 0 \} \quad (48)$$

$[K]$ is the stiffness matrix calculated in small-displacements range, $[G]$ is the geometric stiffness matrix corresponding to a reference load, " λ " is the eigenvalue, that is the load factor to multiply to the reference load to obtain the critical value. As is written, the equation system appears as an eigenvalues determination problem, then for found some values of " λ ",

$$\det([K] - \lambda[G]) = 0 \quad (49)$$

4 RESULTS AND DISCUSSION

Although the Rayleigh-Ritz method in Area coordinate presented in this paper can be used to study buckling of general triangular plates, we will concentrate our analysis on right-angled and isosceles orthotropic plates subjected to in-plane compressive and shear load with various boundary conditions. To describe the Boundary conditions in a composite thin plate, we use letters F for free, S for simply supported and C for clamped edges. Consider an orthotropic triangular plate with length a , a vertex angle α_0 , uniform thickness t , the modulus of elasticity E_1, E_2 , and Poisson's ratio ν_{12}, ν_{21} , as shown in Fig. 2. This figure shows the selected right-angled and isosceles composite triangular thin plate studied in this paper.

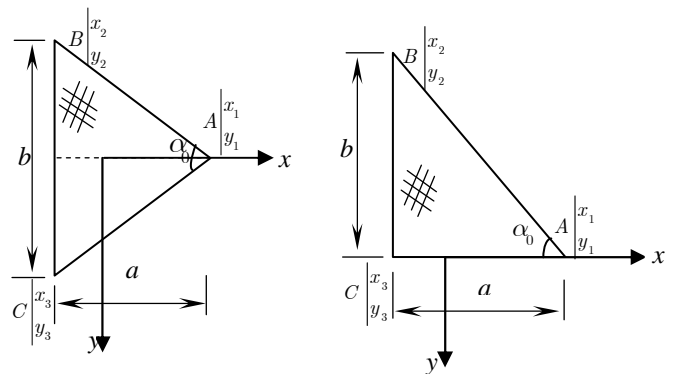
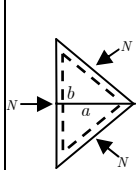
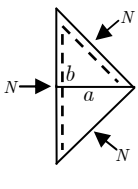


Fig. 2. Composite isosceles and right-angled triangular plate

4.1 Validation

As the Rayleigh-Ritz method used in this study is an approximate numerical approach, convergence and comparison studies are essential to ensure the correctness and convergence of the buckling results. These results are given in Table. I and Table. II.

	Table. I. Comparison of the buckling factor ($\lambda_{cr} = \bar{N}b^2/\pi^2D$) of the isotropic triangular plate			
	b/a	1	$2/\sqrt{3}$	2
Ref [14]	45.827	52.637	98.696	
Present work	46.142	52.666	99.000	

	Table II. Comparison of the buckling factor $(\lambda_{cr} = \bar{N}b^2/\pi^2D)$ of the isotropic triangular plate		
	b/a	1	$2/\sqrt{3}$
	Ref [14]	6.609	8.371
	Present work	6.626	8.386

4.2 Effect of Parameters on Buckling Factors

To take some results for more deliberation of present formulation, at this step we consider orthotropic isosceles and right-angled triangular plates with following data and specifications,

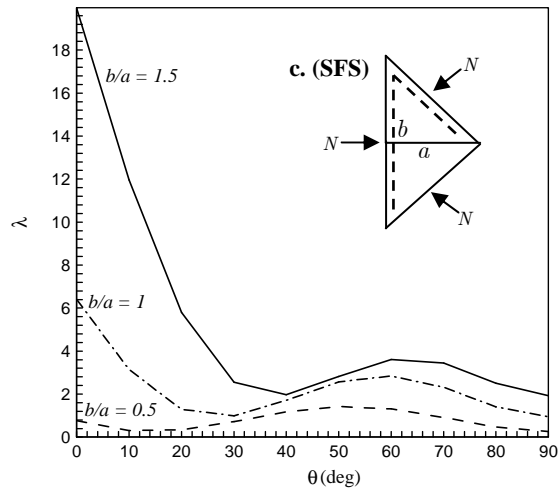
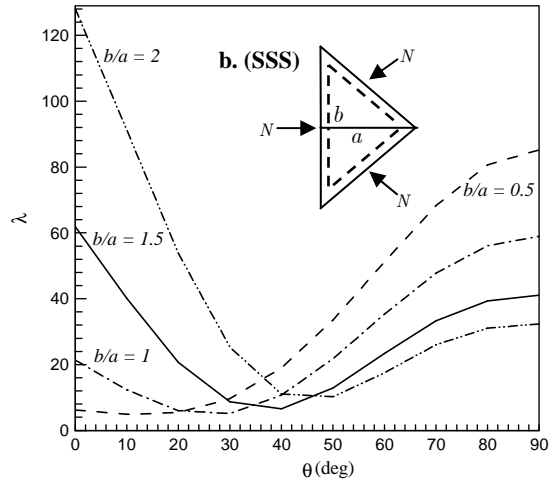
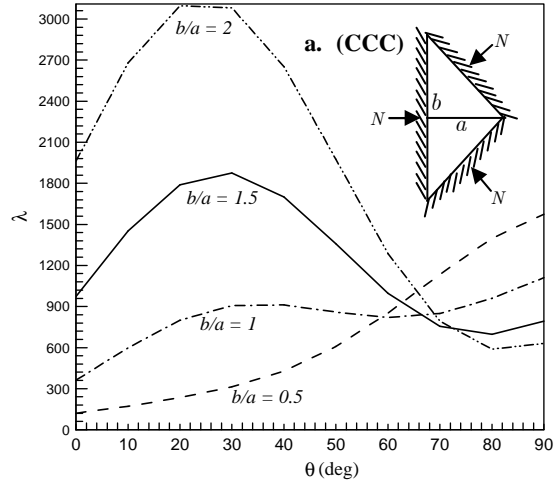
$$E_1 = 155Gpa, E_2 = 8.07Gpa, G_{12} = 4.55Gpa$$

$$v_{12} = 0.22, v_{21} = 0.22, t = 0.001016m$$

and so for plate geometry we consider $a=1(m)$, for instance. Now we determine the critical buckling loads in terms of non-dimensional parameter, $\lambda = \bar{N}b^2/E_2t^3$, where \bar{N} is the critical buckling compressive or shear loads. Boundary conditions are defined as C=Clamped, S=Simple Support and F=Free Support Conditions.

In Figures. 3a – 3c the buckling factors for isosceles triangular plates for different combinations of edge conditions, fiber orientations and width-to-height ratios, $b/a = 0.5, 1, 1.5$ and 2 are presented for the support conditions (CCC-SSS-SFS-CFC-FCF). The following observations are made from these figures,

- The buckling load factor is higher for BC-a (CCC) for all the width-to-height ratios
- For BC-a (CCC), buckling factor has an increasing trend until $\theta = 25^\circ$ for $b/a=1, 1.5, 2$ and will decrease by increasing θ to $\theta = 65^\circ$. By increasing width-to-height ratios from $b/a=0.5$ to $b/a=2$, the buckling factor increased until $\theta = 65^\circ$
- For BC-b (SSS), buckling factor has a decreasing trend until $\theta \approx 35^\circ$ and will increase by increasing θ .
- For BC-d (CFC), buckling factor has an increasing trend for $b/a=0.5, 1$ and decreasing trend for $b/a=1.5, 2$ until $\theta = 70^\circ$.
- For BC-e (FCF), for width-to-height ratios of $b/a=0.5, 1, 1.5$ and 2 , buckling load factor increases for $\theta = 0^\circ$ to $\theta = 75^\circ, 60^\circ, 50^\circ, 45^\circ$, then it decreases.



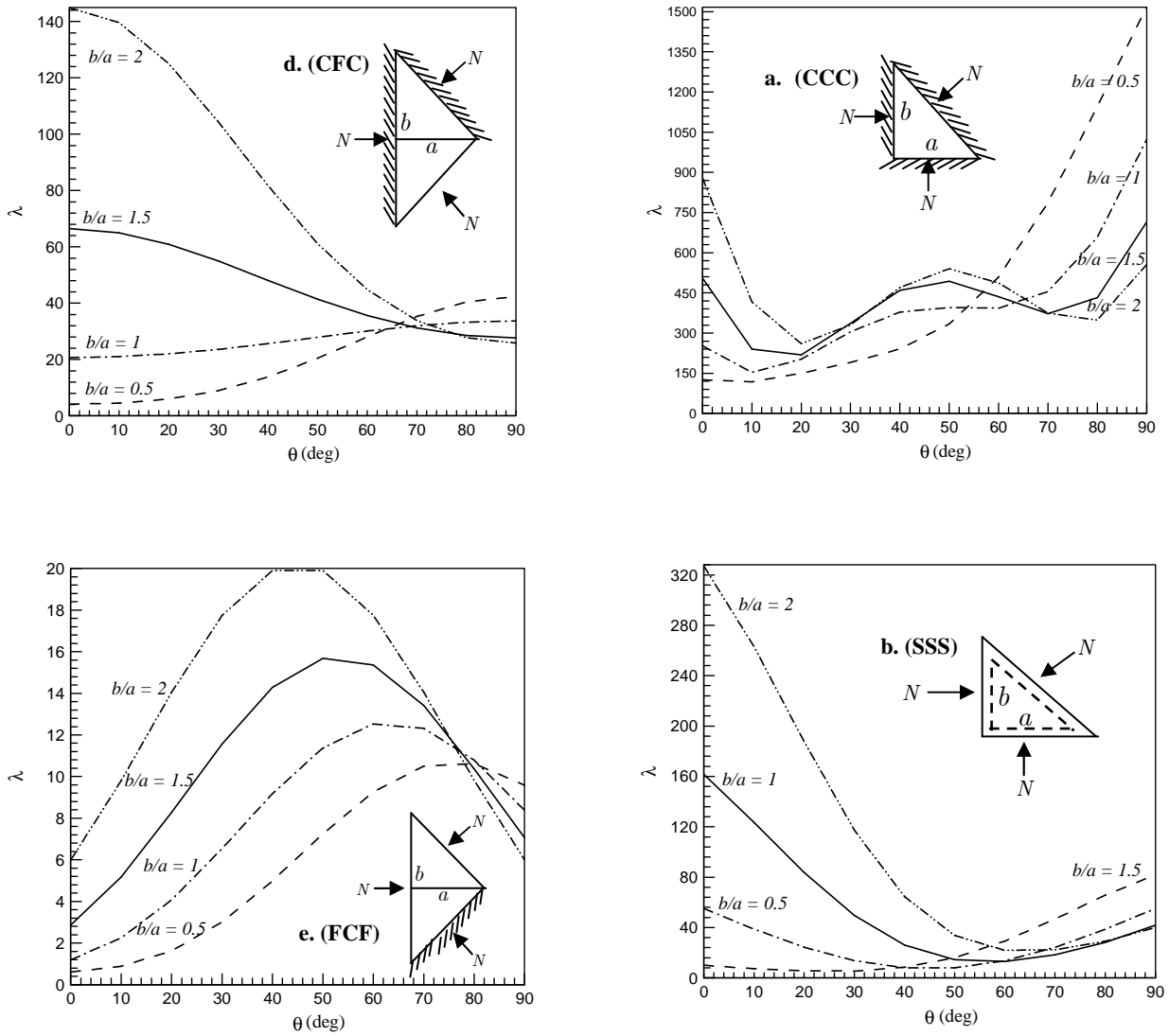
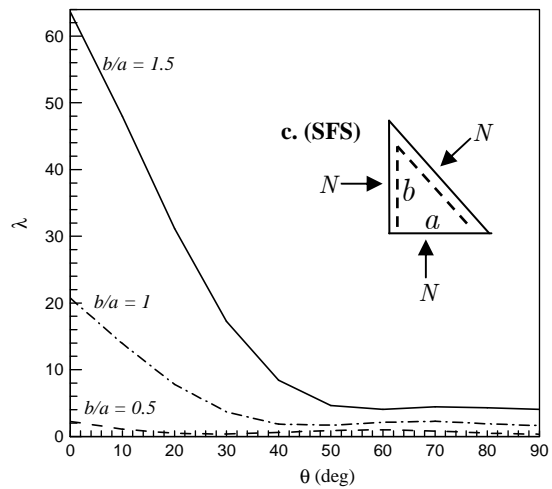


Fig. 3. Variation of buckling factor for isosceles triangular plate with respect to fiber orientation for different width-to-height (b/a) and different boundary conditions

In Figures. 4a – 4d the buckling factors for right-angled triangular plates for different combinations of edge conditions, fiber orientations and width-to-height ratios, $b/a = 0.5, 1, 1.5$ and 2 are presented for the support conditions (CCC-SSS-SFS-CFC). The following conclusions are made from these figures,

- The buckling load factor is higher for BC-a (CCC) for all the width-to-height ratios
- For BC-a (CCC), maximum and minimum buckling load factors at $\theta = 90^\circ$ are seen in $b/a=0.5$ and 2 .
- For BC-b (SSS), buckling factor decreases for $\theta = 0^\circ$ to $\theta \approx 65^\circ$ becoming minimum at $\theta \approx 65^\circ$ and then increases for $\theta \approx 65^\circ$ to $\theta = 90^\circ$ for $b/a=1, 1.5, 2$.
- For BC-c (SFS), buckling factor decreases for $\theta = 0^\circ$ to $\theta \approx 50^\circ$ and then become constant for $b/a=1, 1.5$.



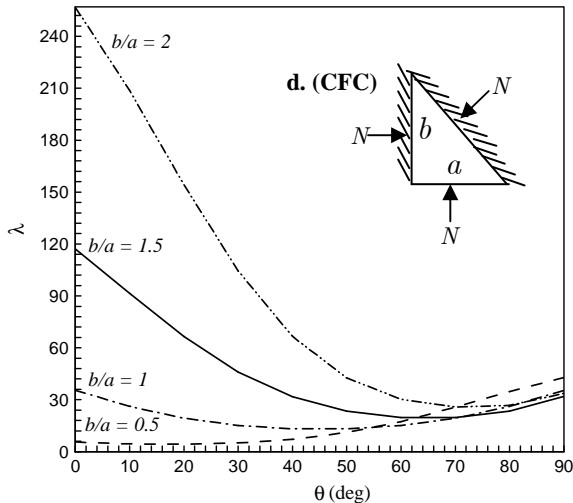


Fig. 4. Variation of buckling factor for right-angled triangular plate with respect to fiber orientation for different width-to-height (b/a) and different boundary conditions

5 CONCLUSION

This paper presents a research about the buckling of composite triangular plates. The total energy functional for a general composite triangular plate is derived, and the eigenvalue equation for elastic buckling of the plate is obtained through the application of the Rayleigh-Ritz method. To this end, computer code has been developed to simulate the buckling behavior of the composite triangular plate model. The new sets of buckling results are by far the most comprehensive and accurately obtained. Convergence and comparison studies are carried out to verify the validity and accuracy of the solution method. Extensive first-known buckling solutions for several selected right-angled and isosceles composite triangular plates are presented in the paper. The influence of the fiber orientation and width-to-height ratios on the buckling behavior of the plates is examined.

6 REFERENCES

[1] Ugural A.C., "Stresses in Plates and Shells" , 2nd., WCB/McGraw-Hill, 1999.
 [2] Timoshenko S., Woinowsky-Krieger S., "Theory of Plates and Shell", 2nd ed., McGraw-Hill, 1959.
 [3] Tung T.K., Surdenas J., "Buckling of rectangular orthotropic plates under biaxial loading", Journal of Composite Materials, Vol.21, No.2, 1987, pp. 124-128.

[4] Wang, J. T.S., Biggers S.B., Dickson J.N., "Buckling of composite plates with a free edge in edgewise bending and compression", AIAA journal, Vol.22, No.3, 1984, pp. 394-398.
 [5] Farshad M., Ahmadi G., "Perturbation solution to the problems of general orthotropic rectangular plates", Iranian Journal of Science and Technology, Vol.1, No.2, 1971, pp. 147-162
 [6] Whitney J.M., Leissa A.W., Biggers S.B., Dickson, J.N., "Analysis of a simply supported laminated anisotropic rectangular plate" , AIAA journal, Vol.8, No.1, 1970, pp. 28-33.
 [7] Woinowsky-Krieger, S. "Berechnung der ringsum frei aufliegenden gleichseitigen dreiecksplatte", Ing. Archiv, 1933. 4, 54-262.
 [8] Burchard, W., "Beulspannungen der quadratischen platte mit schrageife under druck bzw. Schub", Ing Archiv. 1937, 21(107), 332-348.
 [9] Wakasugi. S., " Buckling of a simply supported equilateral triangular plate", Trans. Japan. Soc. Mech. Eng. 1960, 26, (164), 538-544.
 [10] Wakasugi. S., " Buckling of a clamped equilateral triangular plate under uniform compression", Trans. Japan. Soc. Mech. Eng. 1961, 27 (179), 1010-1017.
 [11] Conway. H. D. and Leissa. A. W., "A method for investigating certain eigenvalue problems of the buckling and vibration of plates", J. Appl. Mech. 1960, 27, 557-558.
 [12] Tan, H. K. V., Bettess, P., Bettess, J. A. "Elastic buckling of isotropic triangular flat plates by finite elements. Appl. Math. Modelling 7, 311-316 (1983).
 [13] Tan, H. K. V., "Elastic buckling of isotropic triangular flat plates by finite elements", Proc. Inst. Civil Engineers 77, 13-21(1984).
 [14] Wang, C.M., Liew, K.M., "Buckling of triangular plates under uniform compression". Eng. Struct. 16, 43-50 (1994)

International Journal of GEOMATE, June, 2012, Vol. 2, No. 2 (Sl. No. 4), pp. 253-260

MS No.3h received July 28, 2011, and reviewed under GEOMATE publication policies.

Copyright © 2012, International Journal of GEOMATE. All rights reserved, including the making of copies unless permission is obtained from the copyright proprietors. Pertinent discussion including authors' closure, if any, will be published in the June 2013 if the discussion is received by Dec. 2012.

Corresponding Author: Touraj-Farsadi